

Characterization of the Mixed Radiation Field Produced by Carbon and Oxygen Ion Beams of Therapeutic Energy: A Monte Carlo Simulation Study

C K Ying¹, David Bolst², Anatoly Rosenfeld², Susanna Guatelli²

¹Oncological and Radiological Science Cluster, Advanced Medical and Dental Institute, Universiti Sains Malaysia, Kepala Batas, Pulau Pinang, Malaysia,

²Centre of Medical Radiation Physics, University of Wollongong, NSW, Australia

Abstract

Purpose: The main advantages of charged particle radiotherapy compared to conventional X-ray external beam radiotherapy are a better tumor conformality coupled with the capability of treating deep-seated radio-resistant tumors. This work investigates the possibility to use oxygen beams for hadron therapy, as an alternative to carbon ions. **Materials and Methods:** Oxygen ions have the advantage of a higher relative biological effectiveness (RBE) and better conformality to the tumor target. This work describes the mixed radiation field produced by an oxygen beam in water and compares it to the one produced by a therapeutic carbon ion beam. The study has been performed using Geant4 simulations. The dose is calculated for incident carbon ions with energies of 162 MeV/u and 290 MeV/u, and oxygen ions with energies of 192 MeV/u and 245 MeV/u, and hence that the range of the primary oxygen ions projectiles in water was located at the same depth as the carbon ions. **Results:** The results show that the benefits of oxygen ions are more pronounced when using lower energies because of a slightly higher peak-to-entrance ratio, which allows either providing higher dose in tumor target or reducing it in the surrounding healthy tissues. It is observed that, per incident particle, oxygen ions deliver higher doses than carbon ions. **Conclusions:** This result coupled with the higher RBE shows that it may be possible to use a lower fluence of oxygen ions to achieve the same therapeutic dose in the patient as that obtained with carbon ion therapy.

Keywords: Carbon ions, charged particle therapy, Geant 4, Monte Carlo simulation, oxygen ions

Received on: 02-05-2019

Review completed on: 14-08-2019

Accepted on: 27-08-2019

Published on: 11-12-2019

INTRODUCTION

Proton and carbon ion therapy are two types of hadron therapy which have been increasingly used in recent years for cancer treatment, with many new facilities under construction or planned for the near future.^[1-6] One of the main advantages of charged particle radiotherapy compared to conventional X-ray external beam radiotherapy is a better dose conformality. Heavy charged particles deposit the major part of their energy at the end of their range, at the Bragg peak. This allows to provide greater dose in the tumor while sparing the surrounding healthy tissues. For this reason, hadron therapy is particularly suitable for deep-seated tumors.^[7,8]

Currently, hadron therapy centers in the United States offer only proton beams.^[9] Carbon ion therapy is currently available in Japan, for example, at the heavy-ion medical accelerator (HIMAC) at the National Institute of Radiological

Sciences (NIRS, Chiba), and in Europe, for example, the Heidelberg Ion-Beam Therapy Center (HIT).

Oxygen ions are currently considered as a potential alternative to carbon ions. Because of their mass, oxygen ions have less lateral scattering. This contributes favorably to the tumor conformality. The high linear energy transfer (LET) of oxygen ions when compared to carbon ions is associated with higher radiobiological effectiveness (RBE) which translates to better treatment effectiveness when treating hypoxic tumors.^[10-12] Kurz *et al.* published the results of the first experimental-based study of an oxygen ion beam in 2012.

Address for correspondence: Dr. C K Ying,

Oncological and Radiological Science Cluster, Advanced Medical and Dental Institute, Universiti Sains Malaysia, 13200, Kepala Batas, Pulau Pinang, Malaysia.

E-mail: ckying7@usm.my

This is an open access journal, and articles are distributed under the terms of the Creative Commons Attribution-NonCommercial-ShareAlike 4.0 License, which allows others to remix, tweak, and build upon the work non-commercially, as long as appropriate credit is given and the new creations are licensed under the identical terms.

For reprints contact: reprints@medknow.com

How to cite this article: Ying CK, Bolst D, Rosenfeld A, Guatelli S. Characterization of the mixed radiation field produced by carbon and oxygen ion beams of therapeutic energy: A Monte Carlo simulation study. *J Med Phys* 2019;44:263-9.

Access this article online

Quick Response Code:



Website:
www.jmp.org.in

DOI:
10.4103/jmp.JMP_40_19

In particular, they measured the depth-dose distributions of oxygen ions beams at the HIT. Their work contributed to the development of a preclinical oxygen ion-beam experimental database, already being used in research purpose treatment planning systems to support radiobiological experiments with oxygen ion beams at HIT.^[13] With respect to carbon ions, oxygen ions produce more nuclear fragments, which need to be investigated, as they can affect the RBE and the sensitivity to oxygenation.^[14] In addition, the dose due to such fragments needs to be investigated not only in-field but also out-of-field, laterally and beyond the Bragg peak, to study the effect of the mixed radiation field in the healthy tissues surrounding the tumor target.

The possible use of helium and oxygen ions in hadron therapy has recently gained more attention. Yu-Shen *et al.* investigated the longitudinal and lateral dose profiles and RBE produced by protons, α particles, and carbon ions.^[15] Tessonnier *et al.* studied the basic dosimetric features of the different ions, including oxygen ions by experiments.^[16] Mattei *et al.* studied the prompt gamma-ray emission by the interaction of helium, carbon, and oxygen ion beams with a polymethyl methacrylate phantom.^[17] Burigo *et al.* compared the dose distributions and cell survival fractions for various incident ions. They concluded that the optimal projectile depends on the location of the tumor and on the radiosensitivity of the irradiated tissues.^[18]

This work compares the dose produced in a water phantom by an oxygen ion (^{16}O) beam with respect to a carbon (^{12}C) ion beam. This work has been done by using Geant4 Monte Carlo simulations.^[19]

MATERIALS AND METHODS

Geant4 Monte Carlo simulation toolkit, from the European Organization for Nuclear Research, CERN (Geneva, Switzerland) version 4.10.1.p01 was used to model and compare the radiation fields produced by carbon and oxygen ion beams in a 30 cm \times 30 cm \times 30 cm water phantom. A 5 cm \times 5 cm square beam is simulated normally incident on the water phantom with an air gap of 30 cm between the particle source and the surface of the phantom. Carbon beams were generated with energies of 162 MeV/u and 290 MeV/u, which are typical energies used in carbon ion therapy at HIMAC.^[20] The simulations were repeated substituting the carbon with an oxygen beam with energies 192 MeV/u and 345 MeV/u (corresponding to ranges of approximately 60 mm and 161 mm in water, similar to the carbon ion beam).

The G4EmStandardPhysics_Option3 and QGSP_BIC_EMY Geant4 Physics List were adopted to model the electromagnetic and hadronic physics interactions.^[21] The results obtained with oxygen and carbon ion beams were compared in terms of dose distribution in the phantom and peak to entrance dose ratio. The contribution to dose deriving from secondary fragments was studied as well. 10^6 histories were simulated for each configuration to obtain a statistical uncertainty within 1%, with the corresponding confidence interval of the uncertainty being 95%.

RESULTS AND DISCUSSION

Figure 1 shows the energy deposited in the phantom per incident particle in the case of incident 162 MeV/u ^{12}C and 192 MeV/u ^{16}O ions. The ^{16}O beam produces approximately 50% higher energy deposition than the ^{12}C beam at the entrance, at 2 mm depth from the surface of the phantom. At the Bragg peak, approximately at 60-mm depth from the surface of the phantom, the ^{16}O beam produces approximately 60% higher energy deposition than the ^{12}C beam. In addition, the ^{16}O beam produces 150% higher energy deposition tail just after the Bragg peak (at 2-mm depth after the Bragg peak). The peak-to-entrance ratio is 9.0 for the ^{16}O , just slightly higher than that of ^{12}C beams, which is 8.5.

Figure 2 shows the energy deposition per incident particle, for ^{12}C and ^{16}O beams with energies 290 MeV/u and 345 MeV/u, respectively. In this case, it was found that the dose at the entrance (at 2-mm depth from the surface of the phantom) and at the Bragg peak (approximately at 60-mm depth), produced by the ^{16}O ions was about 60% higher than in the case of the ^{12}C beam. Still, the dose at the distal edge of the Bragg peak (2 mm after the Bragg peak) is 140% higher in the case of irradiation with oxygen beams. This is a shortcoming of oxygen ions (organs at risk may be located at the distal edge) and should be taken into consideration if switching from carbon ions to oxygen ions in hadron therapy. The peak-to-entrance ratio for ^{16}O and ^{12}C beams is found to be 5.4 and 5.8, respectively

These results are in agreement with Francesco *et al.*, who compared absolute dose per unit fluence produced by four different types of ion species (protons and helium, carbon and oxygen ions).^[12] Higher peak-to-entrance ratio means that the dose may be increased in the tumor target or reduced in the surrounding healthy tissues of the patient, in front of the tumor. Results of the current study show that increasing the beam energy decreases the peak-to-entrance ratio for both oxygen and carbon ions. In terms of peak-to-entrance

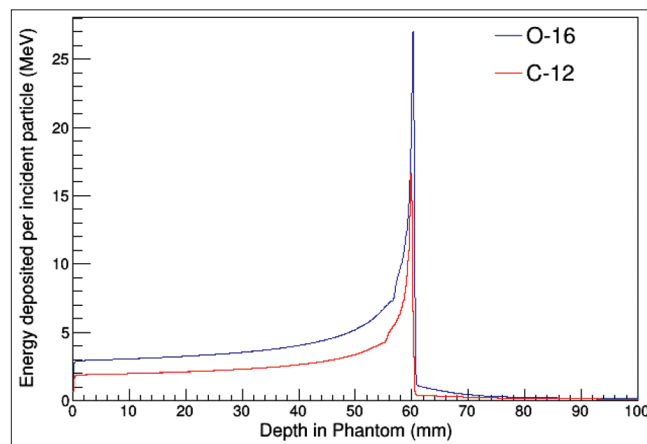


Figure 1: Depth-energy deposition profile in water for 162 MeV/u ^{12}C (red) and 192 MeV/u ^{16}O beams (blue) per incident particle, with 30 cm \times 30 cm \times 0.01 cm voxels (0.01 cm along the direction of the beam)

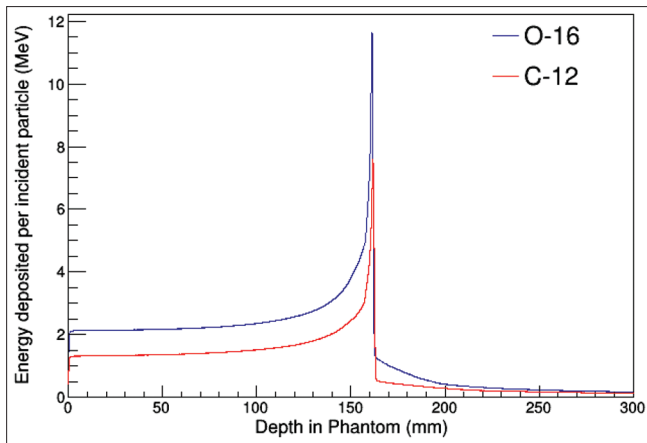


Figure 2: Depth-energy deposition profile in water for 290 MeV/u ^{12}C (red) and 345 MeV/u ^{16}O beams (blue) per incident particle, with $30\text{ cm} \times 30\text{ cm} \times 0.01\text{ cm}$ voxels (0.01 cm along the direction of the beam)

ratio, the benefits of oxygen ions are more pronounced at lower energy.

Figure 3 shows the energy deposited by the secondary radiation field produced by the incident carbon ions (162 MeV/u) and oxygen ions (192 MeV/u) along the depth in the phantom. The results are normalized per incident primary. The results clearly illustrate that fragmentation has a more prominent role in the case of the oxygen beam, as expected, in all regions (i.e., the plateau region, the Bragg peak position, and beyond the Bragg peak). The dose contribution of individual secondary fragment species with higher production yield is presented in Figure 4. Both hydrogen and helium fragments have a longer range than incident ions and heavier fragments, and they contribute most to the dose beyond the Bragg peak.

It can be observed that secondary protons, produced by incident oxygen ion beams deposit more energy than in the case of carbon ions beams in all regions (i.e., the plateau region, the Bragg peak position, and beyond the Bragg peak position). The contribution to the energy deposition deriving from secondary alpha particles is similar along the Bragg peak when comparing oxygen and carbon ion beams. After the Bragg peak, in the case of oxygen ions, alpha particles deposit more energy.

In the case of carbon ion beams, secondary lithium (Li), beryllium (Be), and boron (B) fragments produce more dose in the plateau region and at the Bragg peak position compared to oxygen ions, but, after the Bragg peak, the dose contribution of such fragments is higher with incident oxygen ions. The energy deposition contribution of secondary nitrogen (N) fragments produced by primary oxygen ions is dominant everywhere along the Bragg peak.

Lateral dose distributions for several selected secondary fragments produced by incident oxygen and carbon ions have been compared. Figure 5 shows the results for protons (P) and helium (He), lithium (Li) and boron (B) ion fragments produced by incident 162 MeV/u ^{12}C and 192 MeV/u ^{16}O ions. The two-dimensional histogram (normalized per incident

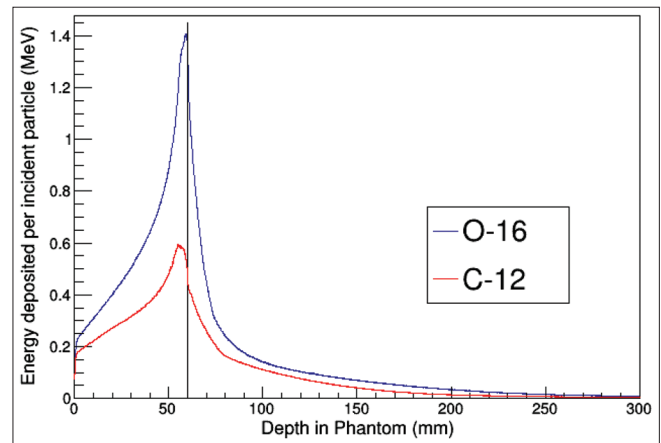


Figure 3: Depth-energy deposition curve produced by the secondary fragments only, with incident ^{16}O (blue) and ^{12}C beams (red) with energy 162 MeV/u and 192 MeV/u. The voxel sizes are $30\text{ cm} \times 30\text{ cm} \times 0.01\text{ cm}$ (0.01 cm along the direction of the beam). The black line at a depth of 60 mm indicates the position of the Bragg peak

primary particle) shows the effects of the scattering outside the radiation field. As expected, the secondary protons scatter more with respect to the other fragments because of their smaller mass. Therefore, lighter fragments contribute more to energy deposition out-of-field. With an increase in the mass of the fragment, the energy is deposited more in a forward direction.

Figures 6-9 show the lateral distribution of the energy deposition per incident oxygen and carbon ion with energy 192 and 162 MeV/u, respectively, including the contributions deriving from secondary protons (P) and lithium ions (Li). Li-ions have been chosen as example of heavier fragment. The comparisons have been done at different depths in the phantom as detailed in the caption of the figures. The plots are normalized per incident primary. The bottom plots indicate the ratio of the dose calculated with incident ^{16}O and ^{12}C beams.

The energy deposition of secondary protons is broader out-of-field with respect to other fragments because protons scatter more due to their smaller mass. Furthermore, the secondary proton beam generated by ^{16}O is slightly broader than ^{12}C at the position 60 mm and 62 mm. The relative energy deposition for ^{16}O is higher than ^{12}C . With an increase of mass, the heavier fragments scatter less and mostly in the forward direction of the incident beam. In the case of secondary Li-ions, the lateral dose distribution for both oxygen and carbon ion are also similar at plateau, at Bragg peak and beyond the Bragg peak. The relative energy deposition for ^{16}O is also higher than ^{12}C .

CONCLUSIONS

This work compared the energy deposition in a water phantom, produced by oxygen ions, proposed as alternative to carbon ions for hadron therapy. The results show that oxygen beams

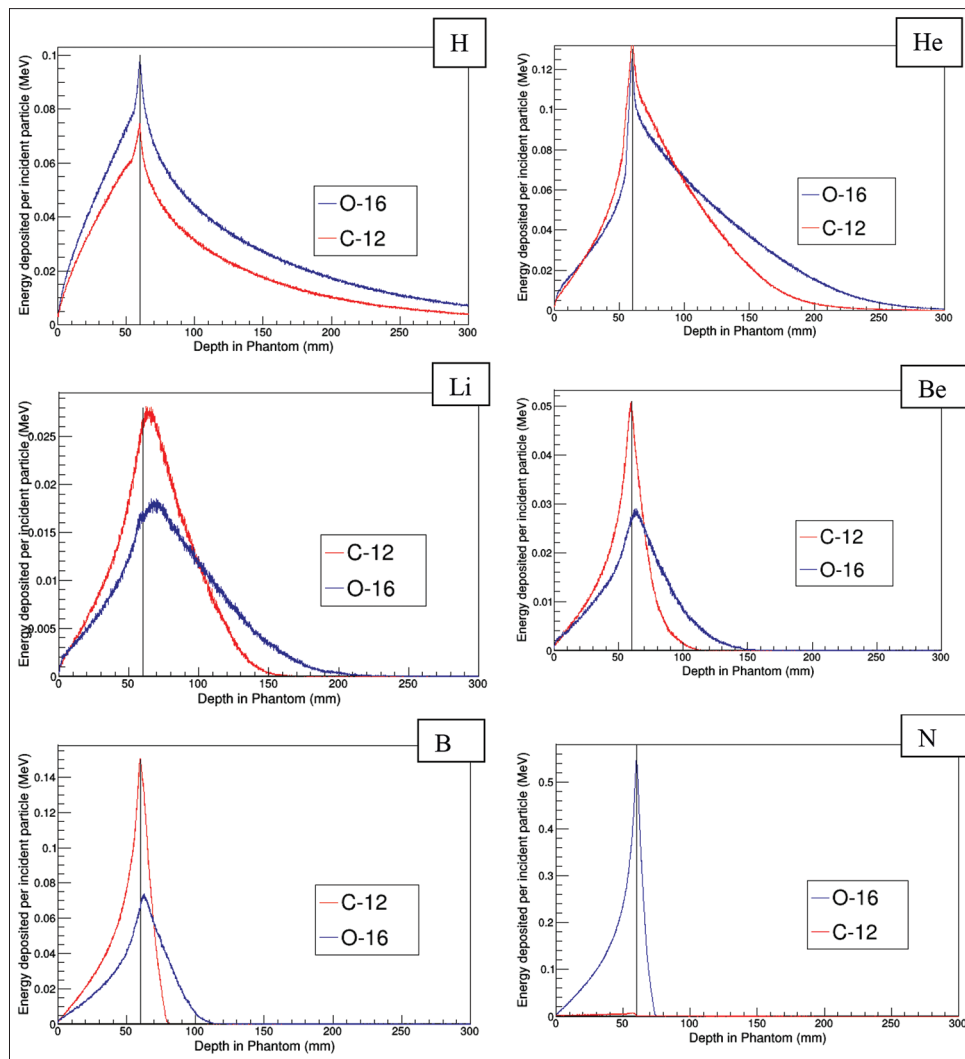


Figure 4: Comparison of depth-energy deposition curves produced by some fragment species, for incident oxygen (red) and carbon (blue) ion beams with energy 162 MeV/u and 192 MeV/u, respectively. The black line at a depth of 60 mm indicates the position of the Bragg peak

are characterized by a higher dose per incident ion and a slightly bigger peak-to-entrance ratio with respect to clinical carbon-ion beams.

With respect to carbon ions, oxygen beams are characterized by higher production of nuclear fragments, which deposit energy beyond the Bragg peak and out-of-field. In addition, such nuclear fragments have an impact on the RBE. These factors have to be carefully taken into account when considering oxygen ions as a possible alternative to carbon therapy.

This work confirms the results of Kumar *et al.*, who investigated various types of ion species using simulation methods and concluded that oxygen ions are the most suitable heavy ions for hadron therapy in addition to carbon ions due to a higher peak-to-entrance ratio and higher energy deposition at the Bragg peak, even though it has a slightly higher entrance dose compared to carbon ion beams.^[22]

In the study of the dependence of the RBE on LET by Francesco *et al.* using research treatment planning system,

the results show the RBE of oxygen was 1.68 and 2.83 at the entrance and at the Bragg peak, respectively and the RBE of carbon was 1.44 and 2.61 at the entrance and at the Bragg peak, respectively. The RBE of oxygen ions is slightly higher than carbon ions at the entrance and at the Bragg peak.^[12] This may be due to the fact that oxygen ions, carrying higher charge, have comparatively higher LET than carbon ions and hence deposit higher dose from fragmentations, translating into higher RBE for oxygen ions than that for carbon ions. Therefore, oxygen beams may be more efficient than carbon ions with hypoxic tumors.^[10-12]

Usually, LET is a key parameter to explain the biological effects induced by charged particles. However, the LET depth-dose profile is also influenced by the types of ions, and hence LET alone cannot explain the differences in their clinical properties. The RBE depends on many parameters, such as LET, fractionation, oxygenation, cell cycle, and endpoint. This study focused on the physical properties of carbon and oxygen ion beams, but biological aspects should

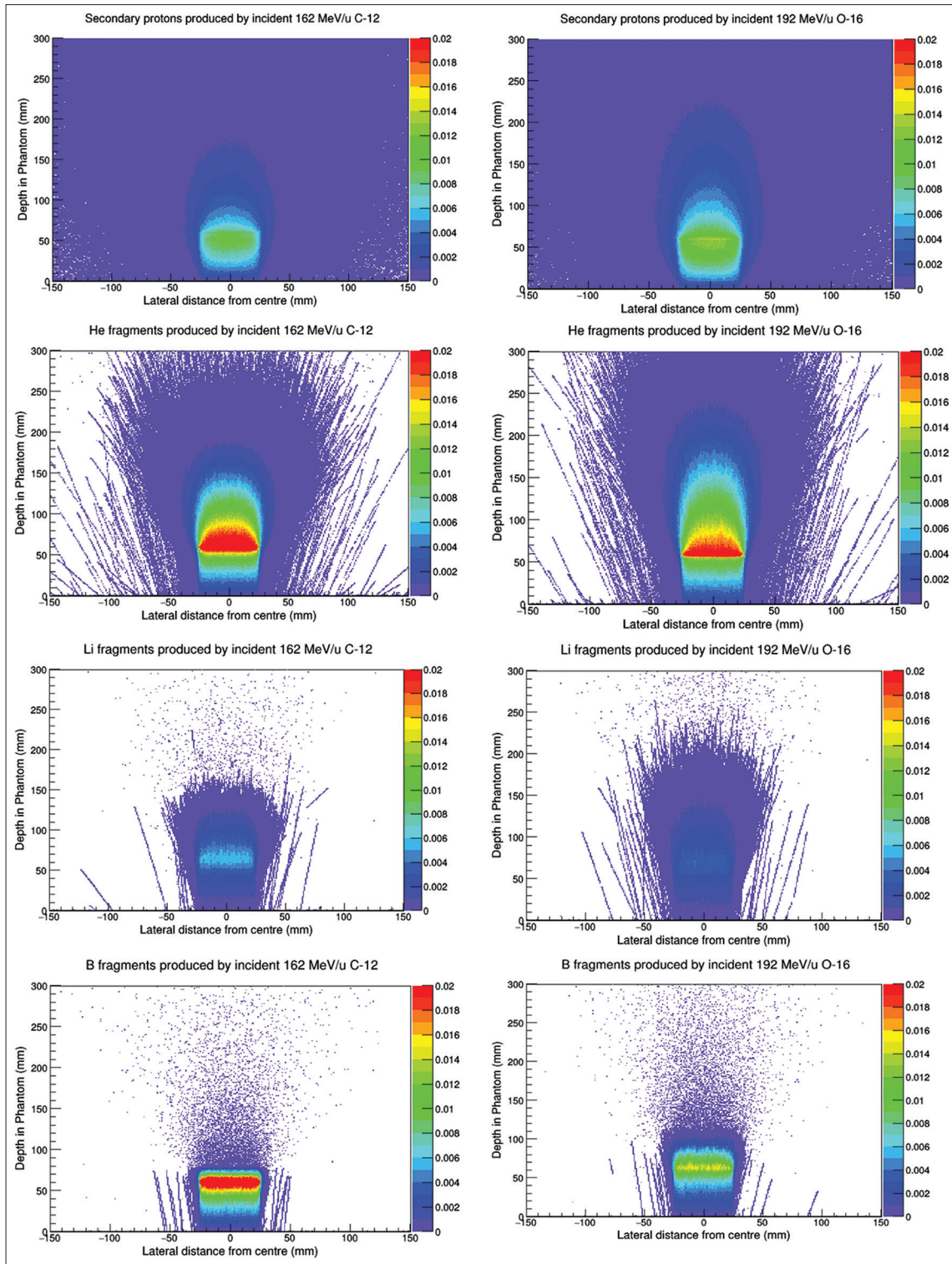


Figure 5: Lateral dose distribution in MeV produced by different fragment species for incident 162 MeV/u carbon ions (left) and 192 MeV/u oxygen ions (right), respectively. The results are normalized per incident primary particle

be considered as well so that the choice of the optimal ion depends on the specific tumor configuration.^[23,24]

Future experimental works will be carried out at the HIMAC, NIRS. Other ions lighter than carbon ions will be studied, especially helium, as helium nuclei are expected to have

favorable dose distributions and a high potential for application in hadron therapy.^[25,26]

Financial support and sponsorship

This work was partially supported by Universiti Sains Malaysia short term grant. No. 304/CIPPT/6315065.

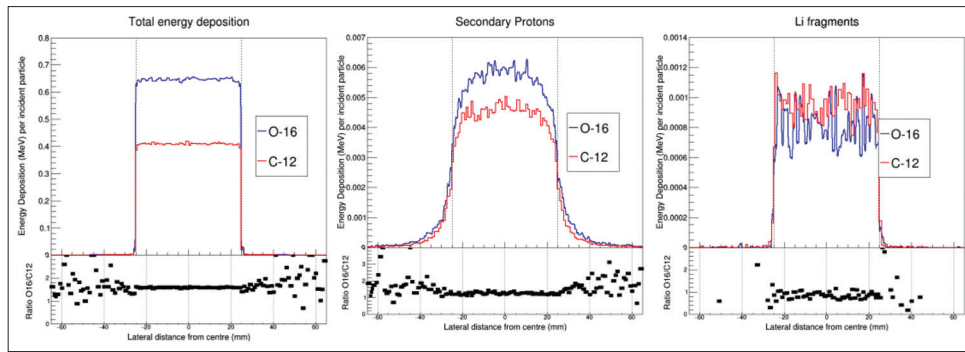


Figure 6: Lateral energy deposition distribution calculated at 15-mm depth in the water phantom (plateau region). Left: total energy deposition. Middle: energy deposition deriving from secondary protons only. Right: energy deposition deriving from secondary lithium ions. The dashed lines at the -25 mm and 25 mm axis X indicates the beam size of 5 cm

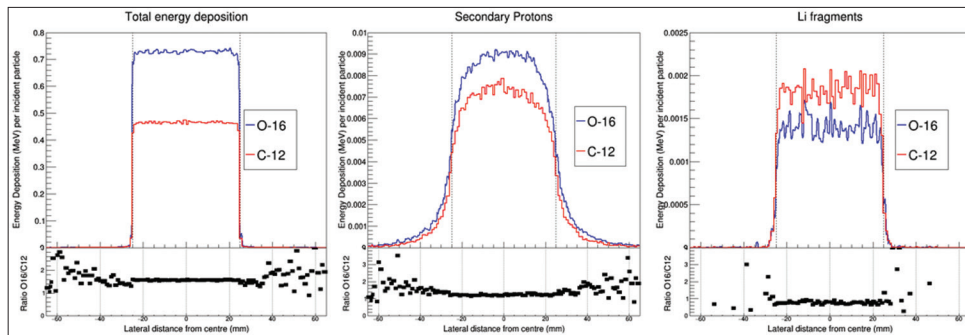


Figure 7: Lateral energy deposition distribution calculated at 30-mm depth in the water phantom (plateau region). Left: total energy deposition. Middle: energy deposition deriving from secondary protons only. Right: energy deposition deriving from secondary lithium ions

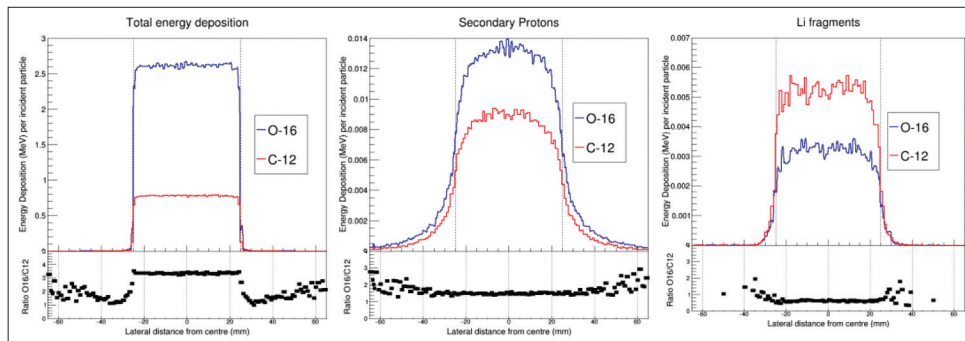


Figure 8: Lateral energy deposition distribution calculated at 60-mm depth in the water phantom (Bragg peak). Left: total energy deposition. Middle: energy deposition deriving from secondary protons only. Right: energy deposition deriving from secondary lithium ions

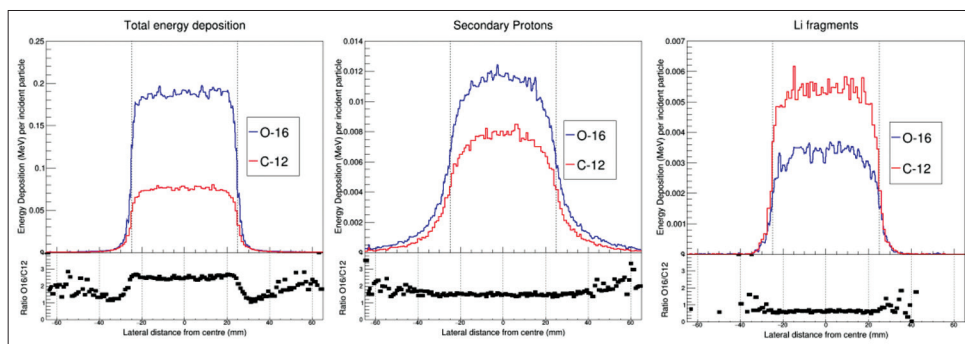


Figure 9: Lateral energy deposition distribution calculated at 62-mm depth in the water phantom (distal edge position). Left: total energy deposition. Middle: energy deposition deriving from secondary protons only. Right: energy deposition deriving from secondary lithium ions

Conflicts of interest

There are no conflicts of interest.

REFERENCES

- Halperin EC. Particle therapy and treatment of cancer. *Lancet Oncol* 2006;7:676-85.
- Kamada T, Tsujii H, Tsuji H, Yanagi T, Mizoe JE, Miyamoto T, *et al.* Efficacy and safety of carbon ion radiotherapy in bone and soft tissue sarcomas. *J Clin Oncol* 2002;20:4466-71.
- Okada T, Kamada T, Tsuji H, Mizoe JE, Baba M, Kato S, *et al.* Carbon ion radiotherapy: Clinical experiences at national institute of radiological science (NIRS). *J Radiat Res* 2010;51:355-64.
- Schulz-Ertner D, Nikoghosyan A, Thilmann C, Haberer T, Jäkel O, Karger C, *et al.* Results of carbon ion radiotherapy in 152 patients. *Int J Radiat Oncol Biol Phys* 2004;58:631-40.
- Terasawa T, Dvorak T, Ip S, Raman G, Lau J, Trikalinos TA, *et al.* Systematic review: Charged-particle radiation therapy for cancer. *Ann Intern Med* 2009;151:556-65.
- Suit H, DeLaney T, Goldberg S, Paganetti H, Clasio B, Gerweck L, *et al.* Proton vs carbon ion beams in the definitive radiation treatment of cancer patients. *Radiother Oncol* 2010;95:3-22.
- Schulz-Ertner D, Tsujii H. Particle radiation therapy using proton and heavier ion beams. *J Clin Oncol* 2007;25:953-64.
- Amaldi U, Kraft G. Radiotherapy with beams of carbon ions. *Rep Prog Phys* 2005;68:1861-82.
- Particle Therapy Facilities in Clinical Operation PTCOG. Available from: <https://www.ptcog.ch/index.php/facilities-in-operation>. [Last accessed on 2019 Apr 30].
- Scifoni E, Tinganelli W, Weyrather WK, Durante M, Maier A, Krämer M, *et al.* Including oxygen enhancement ratio in ion beam treatment planning: Model implementation and experimental verification. *Phys Med Biol* 2013;58:3871-95.
- Bassler N, Toftegaard J, Lühr A, Sørensen BS, Scifoni E, Krämer M, *et al.* LET-painting increases tumour control probability in hypoxic tumours. *Acta Oncol* 2014;53:25-32.
- Francesco T, Emanuele S, Marco D. New ions for therapy. *Int J Part Ther* 2016;2:428-38.
- Kurz C, Mairani A, Parodi K. First experimental-based characterization of oxygen ion beam depth dose distributions at the Heidelberg ion-beam therapy center. *Phys Med Biol* 2012;57:5017-34.
- Weyrather WK, Ritter S, Scholz M, Kraft G. RBE for carbon track-segment irradiation in cell lines of differing repair capacity. *Int J Radiat Biol* 1999;75:1357-64.
- Yu-Shen L, Tsi-Chian C, Ji-Hong H, Chuan-Jong T. Comparisons of longitudinal and lateral dose profiles and relative biological effectiveness for DNA double strand breaks among ^1H , ^4He and ^{12}C beams. *Radiat Phys Chem* 2017;127:169-72.
- Tessonnier T, Mairani A, Brons S, Haberer T, Debus J, Parodi K, *et al.* Experimental dosimetric comparison of ^1H , ^4He , ^{12}C and ^{16}O scanned ion beams. *Phys Med Biol* 2017;62:3958-82.
- Mattei I, Bini F, Collamati F, De Lucia E, Frallicciardi PM, Iarocci E, *et al.* Secondary radiation measurements for particle therapy applications: Prompt photons produced by ^4He , ^{12}C and ^{16}O ion beams in a PMMA target. *Phys Med Biol* 2017;62:1438-55.
- Burigo L, Pshenichnov I, Mishustin I, Bleicher M. Comparative study of dose distributions and cell survival fractions for ^1H , ^4He , ^{12}C and ^{16}O beams using geant4 and microdosimetric kinetic model. *Phys Med Biol* 2015;60:3313-31.
- Agostinelli S, Allison J, Amako K, Apostolakis J, Araujo H, Arce P, *et al.* Geant4 – A simulation toolkit. *Nucl Instrum Methods Phys Res* 2003;506:250-303.
- Torikoshi M, Minohara S, Kanematsu N, Komori M, Kanazawa M, Noda K, *et al.* Irradiation system for HIMAC. *J Radiat Res* 2007;48 Suppl A: A15-25.
- Cirrone GA, Cuttone G, Mazzagila SE. Hadrontherapy: A Geant4-based tool for proton/ion-therapy studies. *Prog Nucl Sci Technol* 2011;2:207-12.
- Kumar A, Jalota S, Gupta R. Simulation of depth-dose distributions for various ions in polyethylene medium. *Adv Space Res* 2012;49:1691-7.
- Remmes NB, Herman MG, Kruse JJ. Optimizing normal tissue sparing in ion therapy using calculated isoeffective dose for ion selection. *Int J Radiat Oncol Biol Phys* 2012;83:756-62.
- Grün R, Friedrich T, Krämer M, Zink K, Durante M, Engenhardt-Cabillic R, *et al.* Assessment of potential advantages of relevant ions for particle therapy: A model based study. *Med Phys* 2015;42:1037-47.
- Rovituso M, Schuy C, Weber U, Brons S, Cortés-Giraldo MA, La Tessa C, *et al.* Fragmentation of 120 and 200 meV $^u\text{-}^{14}\text{He}$ ions in water and PMMA targets. *Phys Med Biol* 2017;62:1310-26.
- Knäusel B, Fuchs H, Dieckmann K, Georg D. Can particle beam therapy be improved using helium ions? – A planning study focusing on pediatric patients. *Acta Oncol* 2016;55:751-9.